Turbulent Mixed Convection from an Isothermal Plate

Aubrey G. Jaffer and Martin S. Jaffer
e-mail: agj@alum.mit.edu

Abstract

The derivation by Jaffer (2023) of the heat transfer formula for natural convection from an external plate revealed a simple relation between heat transfer and fluid flow rates. This relation leads to formulas for turbulent mixed convection from horizontal and vertical plates; these formulas are then combined to predict the mixed convection heat transfer at any plate inclination.

Heat transfer measurements with forced Reynolds number fluid flow rates between 1500 and 50000 were made of each orthogonal combination of plate and fluid flow direction, and of a tilted downward-facing plate. Each data-set matches the present theory with root-mean-squared relative error between 1.4% and 4%.

This research did not receive any specific grant from funding agencies in the public, commercial, or not-for-profit sectors.

Table of Contents

1. Introduction

Natural convection is the flow caused by nonuniform density in a fluid under the influence of gravity. Forced convection is the heat or matter transfer to or from a surface induced by bulk fluid flow parallel to that surface. Mixed convection is the heat or matter transfer when both processes are operating simultaneously. Natural and forced convection are fundamental processes whose combination has applications from engineering to geophysics.

The three modes of forced fluid flow along a flat surface are laminar flow, turbulent flow along a smooth surface, and turbulent flow along a rough surface. Corresponding to each flow mode is a distinct heat transfer formula in Jaffer [1].

Forced convection fluid flow is parallel to the surface. In natural convection the temperature difference between the fluid and surface creates an upward or downward flow, which is not necessarily parallel to the surface.

Natural convection is sensitive to plate inclination, while forced convection is not. Forced convection has different formulas for laminar and turbulent flows, while the same formula governs laminar and turbulent natural convection (Jaffer [2]).

There is a symmetry in external natural convection; a cooled plate induces downward flow instead of upward flow. Flow from a cooled upper face is the mirror image of flow from a heated lower face. Flow from a cooled lower face is the mirror image of flow from a heated upper face.

Sublimation from an upper face is downward convection when the dissolved sublimate is denser than the fluid. The rest of this investigation assumes a plate warmer than the fluid.

1.1 Fluid Mechanics.

In engineering, heat transfer rates for both natural and forced convection are expressed using the average surface conductance $\overline{h}$ with units $\mathrm{W/(m^2 \cdot K)}$.

In fluid mechanics, the convective heat transfer rate is represented by the dimensionless average Nusselt number ($\overline{Nu} \equiv \overline{h}\, L/k$), where k is the fluid's thermal conductivity with units $\mathrm{W/(m \cdot K)}$. The Reynolds

number Re represents the fluid flow rate. The Rayleigh number (Ra) is the impetus to heat flow due to temperature difference and gravity. A fluid's Prandtl number (Pr) is its momentum diffusivity per thermal diffusivity ratio. The system's characteristic length L scales $\overline{Nu}$ and Re; Ra is scaled by L^3; $\overline{h}$ and Pr are independent of L.

1.2 **Combining Transfer Processes.** Formula (1) is an unnamed form for combining functions which appears frequently in heat transfer formulas:

$$F^p = F_1^p + F_2^p \tag{1}$$

Churchill and Usagi [3] stated that such formulas are "remarkably successful in correlating rates of transfer for processes which vary uniformly between these limiting cases." Convection transfers heat (or mass) between the plate and the fluid.

1.3 **The ℓ^p-norm.** Requiring $F_1 \geq 0$ and $F_2 \geq 0$, and taking the pth root of both sides of equation (1) yields a vector-space functional form known as the ℓ^p-norm, which is notated $\|F_1\ ,\ F_2\|_p$:

$$\|F_1\ ,\ F_2\|_p \equiv [\ |F_1|^p + |F_2|^p]^{1/p} \tag{2}$$

Norms generalize the notion of distance. Formally, a vector-space norm obeys the triangle inequality: $\|y\ ,\ z\|_p \leq |y| + |z|$, which holds only for $p \geq 1$. However, $p < 1$ is also useful.

Let $y \geq 0$ and $z \geq 0$. When $p > 1$, the processes compete and $\|y, z\|_p \geq \max(y, z)$; the most competitive is $\|y, z\|_{+\infty} \equiv \max(y, z)$. The ℓ^2-norm is equivalent to root-sum-squared; it models perpendicular competitive processes.

The ℓ^1-norm models independent processes; $\|y, z\|_1 \equiv y + z$.

When $0 < p < 1$, the processes cooperate and $\|y, z\|_p \geq y + z$. Cooperation between conduction and flow-induced heat transfer manifests as the $\ell^{1/2}$-norm in natural convection formula (5).

1.4 **Laminar Flow.** Most published studies of mixed convection investigate laminar flow. It is the nature of turbulent flows that the mixture of laminar and turbulent flows is turbulent. Thus, the natural and forced components of mixed laminar convection must both be laminar if their mixture is to be purely laminar.

Building on the Blasius boundary-layer model of laminar flow (Schlichting [4]), these laminar studies analyze boundary-layer local properties. But natural convection's boundary layer detaches from the center of an upward-facing plate. And the downward-facing boundary layer is split in half. Thus, these prior studies of local laminar convection are limited to a small subset of mixed convection use cases.

Lin, Yu, and Chen [5] presents formulas for local mixed convection for aiding forced flow and opposing forced flow along a vertical plate, and aiding and opposing flow along a downward facing plate. Absent are horizontal forced flow along a vertical plate, and forced flow along an upward facing plate.

Both Fujii and Imura [6] and Aihara, Yamada, and Endö [7] present flow diagrams of a horizontal plate with heated lower face. Unheated fluid below the plate flows horizontally inward. It rises a short distance, flows outward closely below the plate, and flows upward upon reaching the plate edge (see Figure 3). An aiding forced flow does not exist for this configuration.

The local Nusselt number graphs in Lin et al. [5] show many points from numerical simulations of aiding flow over a wide range of Pr, but only four closely spaced opposing flow points. The opposing flow curve ends abruptly because their formula, $\sqrt[4]{1 - X^4}$, has no physical interpretation when $X > 1$.

1.5 **Laminar and Turbulent.** Wang [8] reported local measurements of a horizontal flat plate in a wind tunnel at wind speeds and with temperature differences sufficient to test both laminar and turbulent flows.

Unfortunately, the plate was one of the test chamber walls. The downward facing natural convection flow configuration described earlier would not form because fluid could not rise upon reaching the plate edge. The upward facing flow configuration had its horizontal flows obstructed by the test chamber walls.

2. Materials and Methods

The present apparatus combines an open intake wind-tunnel, software phase-locked loop (PLL) fan control, and a heated aluminum plate centered in the test chamber by a six wire suspension.

This apparatus measured average mixed convection in air with $2300 < Re < 93000$, a 40:1 range. The wind-tunnel chassis (1.3 m × .61 m × .65 m) was small enough to allow positioning in horizontal, vertical, and inclined orientations. An appendix in Jaffer [1] describes the apparatus and measurement methodology with the plate facing down.

Table 1 shows the combinations of flow types and orthogonal orientations. In the "Forced" column, "rough" indicates that the plate was shedding the rough turbulence of formula (10); "smooth" indicates that the flow was primarily smooth turbulent.

Configurations measured by the present apparatus with its 0.305 m square plates are marked with •.

Laminar-only configurations are marked with ∘. These configurations would require a smaller plate and a wind-tunnel capable of reliably delivering laminar flows.

Configurations having turbulent natural convection are marked with ◯. These would require either a larger plate and wind-tunnel or higher plate temperatures than the present apparatus supports.

Table 1 Mixed convective modes

Natural	Forced	Down	Up	Vertical	Opposing	Aiding
laminar	laminar	∘	∘	∘	∘	∘
laminar	smooth	•Figure 5	•Figure 7	•Figure 9	•Figure 11	•Figure 13
laminar	rough	•Figure 6	•Figure 8	•Figure 10	•Figure 12	•Figure 14
turbulent	smooth	◯	◯	◯	◯	◯
turbulent	rough	◯	◯	◯	◯	◯

2.1 Not Empirical.

Empirical theories derive their coefficients from measurements, inheriting the uncertainties from those measurements. Theories developed from first principles derive their coefficients mathematically. For example, the Blasius model of laminar flow coefficient 0.3320+ is the solution of a differential equation (Lienhard and Lienhard [9]). Another example is the heat conduction shape factor for one face of a disk, which is exactly twice its diameter. The present theory derives from first principles; it is not empirical. Each formula is tied to aspects of the plate geometry and orientation, fluid, and flow.

2.2 RMS Relative Error.

Root-mean-squared relative error (RMSRE) provides an objective, quantitative evaluation of experimental data versus theory. It gauges the fit of measurements $g(Re_j)$ to function $f(Re_j)$, giving each of the n samples equal weight in formula (3).

$$\sqrt{\frac{1}{n}\sum_{j=1}^{n}\left|\frac{g(Re_j)}{f(Re_j)}-1\right|^2} \tag{3}$$

$$\text{bias} = \frac{1}{n}\sum_{j=1}^{n}\left\{\frac{g(Re_j)}{f(Re_j)}-1\right\} \qquad \text{scatter} = \sqrt{\frac{1}{n}\sum_{j=1}^{n}\left|\frac{g(Re_j)}{f(Re_j)}-1-\text{bias}\right|^2} \tag{4}$$

Along with presenting RMSRE, charts in the present work split RMSRE into the bias and scatter components defined in formula (4). The root-sum-squared (RSS) of bias and scatter is RMSRE.

3. Natural Convection

Jaffer [2] derived a natural convection formula for external flat plates (with convex perimeter) in any orientation from its analyses of horizontal and vertical plates. This investigation uses the same approach.

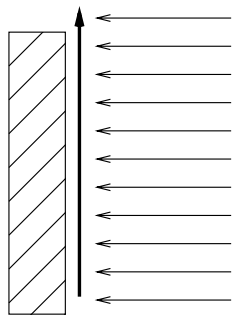

Figure 1 Vertical plate

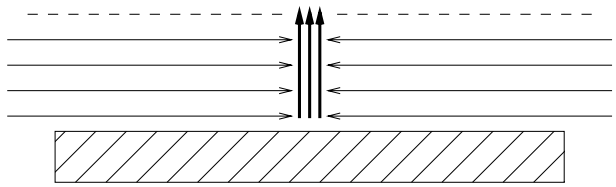

Figure 2 Flow above a heated plate

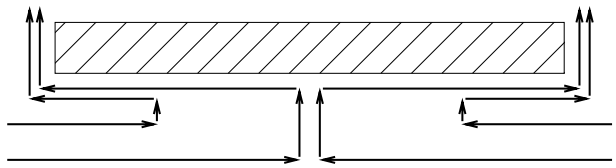

Figure 3 Flow below a heated plate

Figures 1, 2, and 3 show the induced fluid flows around heated vertical and horizontal surfaces. Horizontal flow in Figure 2 is radial, but not in Figure 3. From thermodynamic constraints, Jaffer [2] derives generalized natural convection formula (5) with the parameters specified in Table 2:

- θ is the angle of the plate from vertical;
- The upward-facing characteristic length L^* is the area-to-perimeter ratio of a convex plate;
- The vertical characteristic length L' is the harmonic mean of the perimeter vertical spans;
- The downward-facing characteristic length L_R is the harmonic mean of the perimeter distances to that bisector which is perpendicular to the shortest bisector (1/2 of the shorter side of a rectangle);
- Nu_0 is the fluid's conduction when not moving (static);
- Ra' is computed with vertical L'; $Ra^* = Ra'\,[L^*/L']^3$; $Ra_R = Ra'\,[L_R/L']^3$;
- E is the count of 90° changes in direction of fluid flow;
- B is the sum of the mean lengths of flows parallel to the plate divided by L;
- C is the plate area fraction responsible for flow induced heat transfer;
- D is the effective length of heat transfer contact with the plate divided by L;
- The ℓ^p-norm combines the static conduction and induced convective heat flows.

Table 2 Natural convection parameters

Face	θ	L	$\overline{Nu}$	Nu_0	Ra	E	B	C	D	p
up	$-90°$	L^*	$\overline{Nu^*}$	Nu_0^*	Ra^*	1	2	$1/\sqrt{8}$	1	1/2
vertical	0°	L'	$\overline{Nu'}$	Nu_0'	Ra'/Ξ	1	1/2	1/2	1/4	1/2
down	$+90°$	L_R	$\overline{Nu_R}$	$Nu_0'/2$	Ra_R/Ξ	3	4	1/2	2	1

$$\overline{Nu} = \left\| Nu_0\,[1-C],\ \sqrt[2+E]{[C\,D\,Nu_0]^{3+E}\,\frac{2}{B}\,Ra} \right\|_p \tag{5}$$

$$\Xi = \left\| 1\ ,\ \frac{0.5}{Pr} \right\|_{\sqrt{1/3}} \qquad Nu_0^* = \frac{2}{\pi} \qquad Nu_0' = \frac{2^4}{\sqrt[4]{2}\,\pi^2} \tag{6}$$

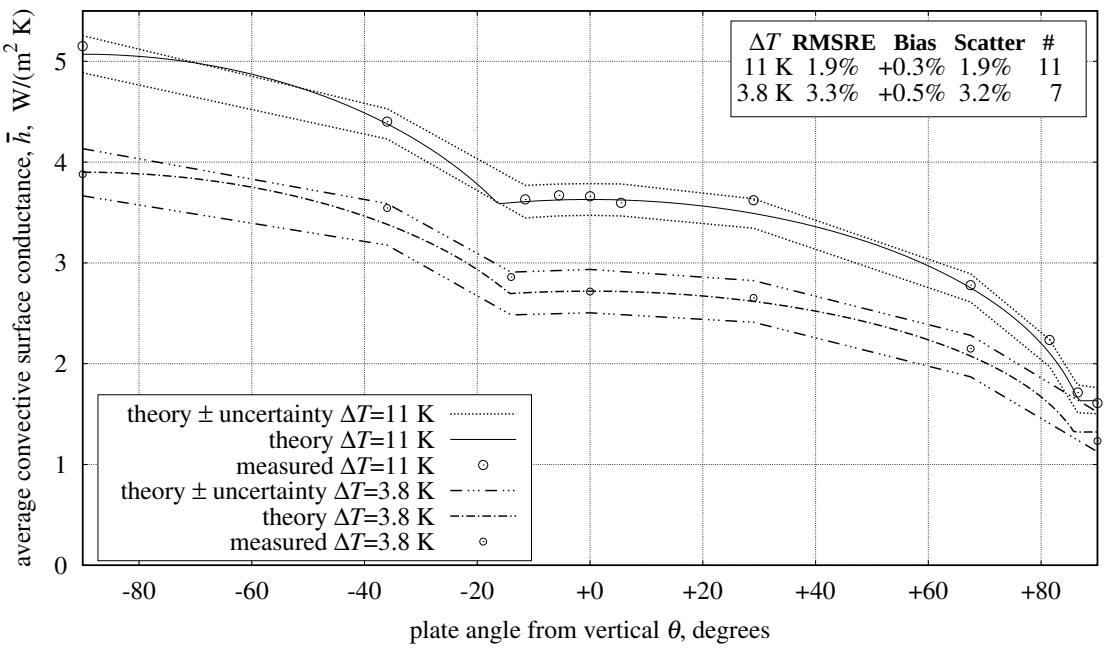

Figure 4 Natural convection versus angle

3.1 **Natural Convection From an Inclined Plate.** Ra is proportional to gravitational acceleration. Following the approach of Fujii and Imura [6], the Ra argument to $\overline{h'}(Ra) \equiv k\,\overline{Nu'}(Ra)/L'$ is scaled by $|\cos\theta|$, modeling the reduced convection of a tilted plate as a reduction in gravitational acceleration. Similarly, the Ra arguments to $\overline{h^*}$ and $\overline{h_R}$ are scaled by $|\sin\theta|$. Upward facing plates are $\theta < 0$.

$$\overline{h} = \begin{cases} \max\left(\overline{h'}(|\cos\theta|\,Ra'/\Xi), \overline{h^*}(|\sin\theta|\,Ra^*)\right) & \theta < 0 \\ \max\left(\overline{h'}(|\cos\theta|\,Ra'/\Xi), \overline{h_R}\,(|\sin\theta|\,Ra_R/\Xi)\right) & \theta \geq 0 \end{cases} \tag{7}$$

An unobstructed plate induces a single steady-state mode of natural convection (face up, down, or vertical). The instances of max() in formula (7) choose the largest surface conductance among these modes.

Note that mode exclusivity does not necessarily hold when flow is (partially) obstructed, such as by side-walls in Fujii and Imura [6] as modeled by Jaffer [2].

3.2 **Rough Natural Convection.** The agreement of rough plate measurements with theory over the 180° range in Figure 4 indicates that, under identical conditions, the average natural convection from a rough plate is the same as the average natural convection from a smooth plate.

3.3 **Effective Vertical Reynolds Number.** From the derivation in Jaffer [2] with $Ra \gg 1$ and $Pr \gg 1$, $\overline{Nu} \approx C\,D\,Nu_0\,Re$. Heat transfer $\overline{Nu'}$ is reduced by the self-obstruction factor $1/\sqrt[3]{\Xi(Pr)}$, which grows with Pr. But heat transfer is not the same as fluid flow, which increases with decreasing Pr. The Ξ^3 factor in formula (8) makes it increase with decreasing Pr. Let Re_N in formula (8) be the Reynolds number associated with the natural convective flow from a vertical plate.

$$Re_N \approx \frac{\overline{Nu}\,\Xi^{2+E}}{Nu_0\,C\,D} = \frac{8\,\overline{Nu'}\,\Xi^3}{Nu'_0} \qquad \overline{Nu'} \gg Nu'_0 \tag{8}$$

4. **Forced Convection**

Forced convection is the heat transfer caused by flow along (and parallel to) a heated (or cooled) plate. The heat transfer rate $\overline{h_F}$ grows with Re, Pr, and k. Its characteristic length L is the length of the plate in the direction of (forced) flow. The remainder of this section has $\overline{h_F}$ details which are not needed to understand how $\overline{h_F}$ and $\overline{h_N}$ combine.

Jaffer [1] derives the comprehensive (laminar and turbulent) average forced convection heat transfer rate, $\overline{h_F}$, of fluid flowing along a smooth, flat, isothermal plate as formula (9).

$$\begin{aligned}
\overline{Nu_F} &= \left\| \overline{Nu_\lambda}(Re), \overline{Nu_\sigma}(Re) - \overline{Nu_\sigma}\left(\|Re, \sqrt{\gamma}\, Re_c\|_{-8/\gamma}\right) \right\|_\gamma \\
\overline{h_F} &\equiv \overline{Nu_F}\, k/L \qquad \gamma = 1 + \exp_2\left(-Pr^{-\sqrt{1/2}}\right) \qquad \exp_2(\varphi) \equiv 2^\varphi \\
\overline{Nu_\sigma}(Re) &= \frac{Nu_0\, Re\, \overline{f_\sigma}(Re)}{\sqrt{3}} \sqrt{\frac{Pr/\sqrt{162}+1}{\sqrt{162}\, Pr\, \overline{f_\sigma}(Re)+1}} \sqrt[3]{\frac{Pr/\Xi}{\|1, 1/Pr\|_3}} \\
\overline{Nu_\lambda}(Re) &= \frac{0.664\, Re\, Pr^{1/3}}{\sqrt{Re}+\sqrt{Re_0}} \qquad \Xi = \left\| 1,\ \frac{0.5}{Pr} \right\|_{\sqrt{1/3}} \qquad Nu_0 = \frac{16}{\pi^2\, \sqrt[4]{2}} \\
\overline{f_\sigma}(Re) &= \frac{\sqrt[3]{2}/3}{\left[\mathrm{W}_0\left(Re/\sqrt{3}\right)-1\right]^2} \qquad Re_c = \frac{\left\|2.629\times 10^6, 1296/Tu\right\|_{-1}}{\sqrt[4]{Pr_\infty}}
\end{aligned} \tag{9}$$

- Re_c is the critical Reynolds number, the Re upper-bound of purely laminar flow.
- Tu is the free-stream turbulence ratio of the bulk flow.
- The fluid's effective Prandtl number $Pr = Pr_w^{1/4}\, Pr_\infty^{3/4}$.
  Pr_w is at plate temperature; Pr_∞ is at bulk flow temperature.
- $Re_0 \approx 600$. Laminar forced convection $\overline{Nu_\lambda}(Re)$ is valid for $Re > 0$.
- W_0 is the principal branch of the Lambert W function; $\mathrm{W}_0(\varphi \exp \varphi) = \varphi$ when $\varphi \geq 0$.

Jaffer [1] also derives the forced convection of fully rough flow from isotropic, periodic roughness:

$$\overline{Nu_F} = \frac{Re\, Pr_\infty^{1/3}\, C_W}{6\, \ln^2(L/\varepsilon)} \qquad C_W = \|1, \varepsilon/L_W\|_{\sqrt{1/2}} \qquad L \gg \varepsilon \tag{10}$$

- ε is the root-mean-squared (RMS) height of roughness.
- L_W is the width of the plate (perpendicular to L).
- The C_W factor increases convection due to roughness seen from the two sides parallel to the flow.

The plateau islands roughness described in Jaffer [1] has formula (10) convection where the local $Re_x < Re_I$. For the purpose of comparison with Re_N formula (8), its effective forced Re is:

$$Re_F(Re) = Re/\exp_{C_W}\left(4\, \exp_4\left(-[Re/Re_I]^4\right)\right) \qquad \exp_b(\varphi) \equiv b^\varphi \tag{11}$$

The corresponding $\overline{Nu}$ transition in Jaffer [1] employs the ℓ^{-4}-norm.

5. **Turbulent Mixed Convection**

The following figures plot $\overline{Nu}$ measurements and theoretical curves versus $10^3 < Re < 10^5$ using logarithmic scales on both axes. Logarithmic scales do not include 0; thus the measurement shown at $Re = 10^3$ are actually natural convection measurements at $Re = 0$.

$-90° \leq \theta \leq +90°$ is the angle of the plate from vertical; $-90°$ is upward facing; $+90°$ is downward.

$0° \leq \psi \leq 180°$ is the angle of the forced flow from the zenith; $\psi = 90°$ is horizontal flow; $\psi = 0°$ is upward. In this investigation forced flow is parallel to the plate; hence, horizontal plates have $\psi = 90°$.

RMSRE is calculated from the measurements between the vertical lines at $Re = 1500$ and $Re = 5 \times 10^4$.

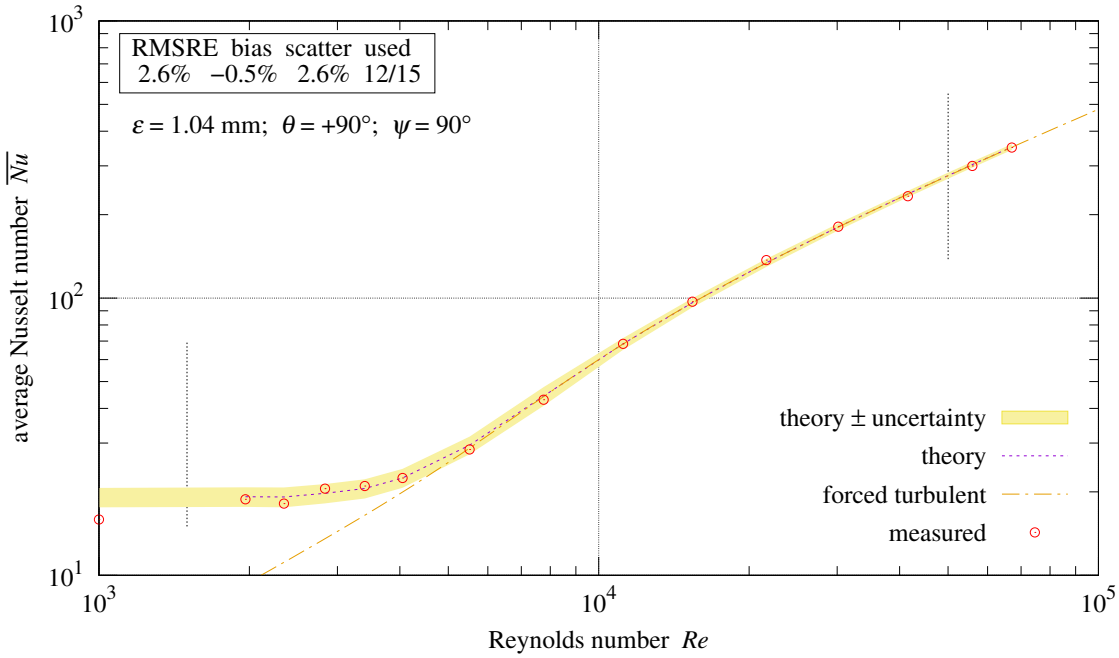

Figure 5 Downward facing plate, smooth turbulence

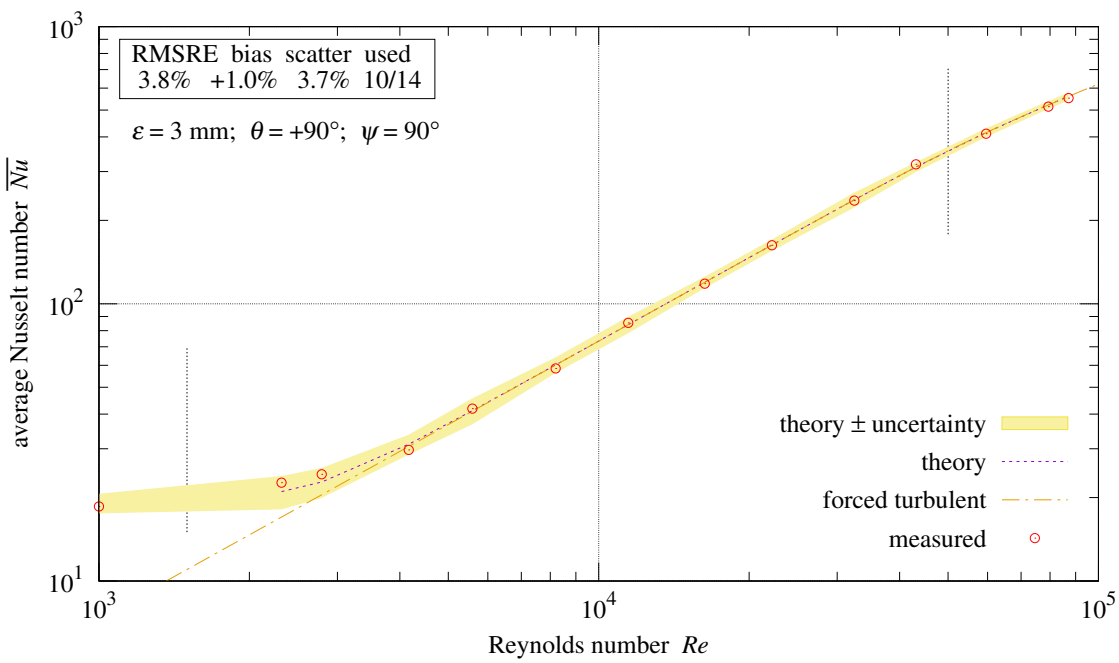

Figure 6 Downward facing plate, rough turbulence

5.1 **Downward Facing Plate.** Figure 3 shows that flow is outward immediately beneath the heated surface. Forced flow parallel to this surface is thus incompatible with downward natural convection $\overline{h_R}$. These two flows will compete for surface area. Table 2 shows that $\overline{Nu_R}$ is proportional to $\sqrt[5]{Ra_R}$, suggesting the ℓ^5-norm for combining $\overline{h_R}$ and $\overline{h_F}$:

$$\overline{h} = \left\| \overline{h_F}, \overline{h_R} \right\|_5 \tag{12}$$

Figures 5 and 6 compare formula (12) with measurements of downward-facing plates shedding forced smooth or forced rough turbulence, respectively.

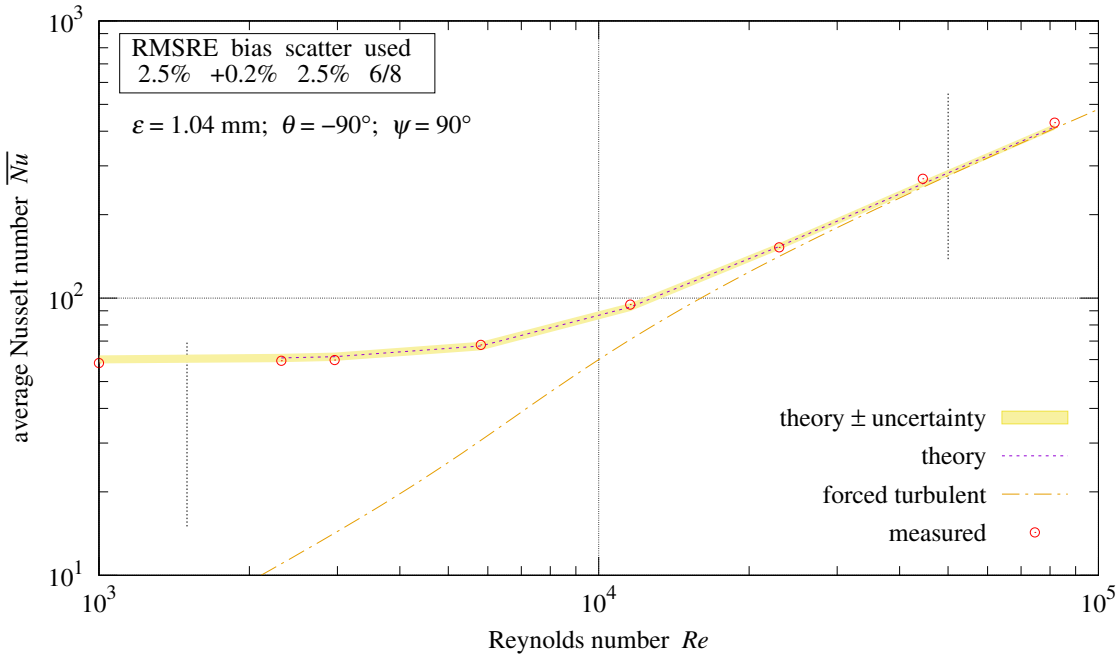

Figure 7 Upward facing plate, smooth turbulence, $\Delta T = 10.3$ K

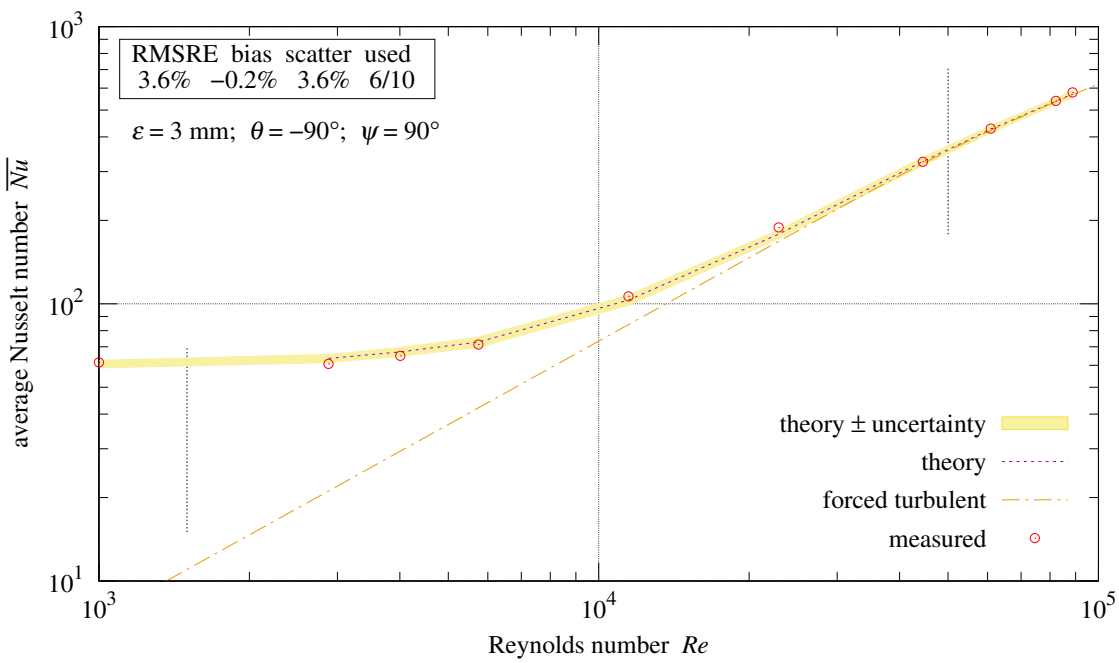

Figure 8 Upward facing plate, rough turbulence

5.2 **Upward Facing Plate.** Figure 2 shows that flow is inward above the heated surface. Forced flow parallel to the surface is thus compatible with upward natural convection $\overline{h^*}$. Their heat flows are perpendicular, suggesting the ℓ^2-norm for combining $\overline{h^*}$ and $\overline{h_F}$:

$$\overline{h} = \left\| \overline{h_F}, \overline{h^*} \right\|_2 \tag{13}$$

Figures 7 and 8 compare formula (13) with measurements of upward-facing plates shedding forced smooth or forced rough turbulence, respectively.

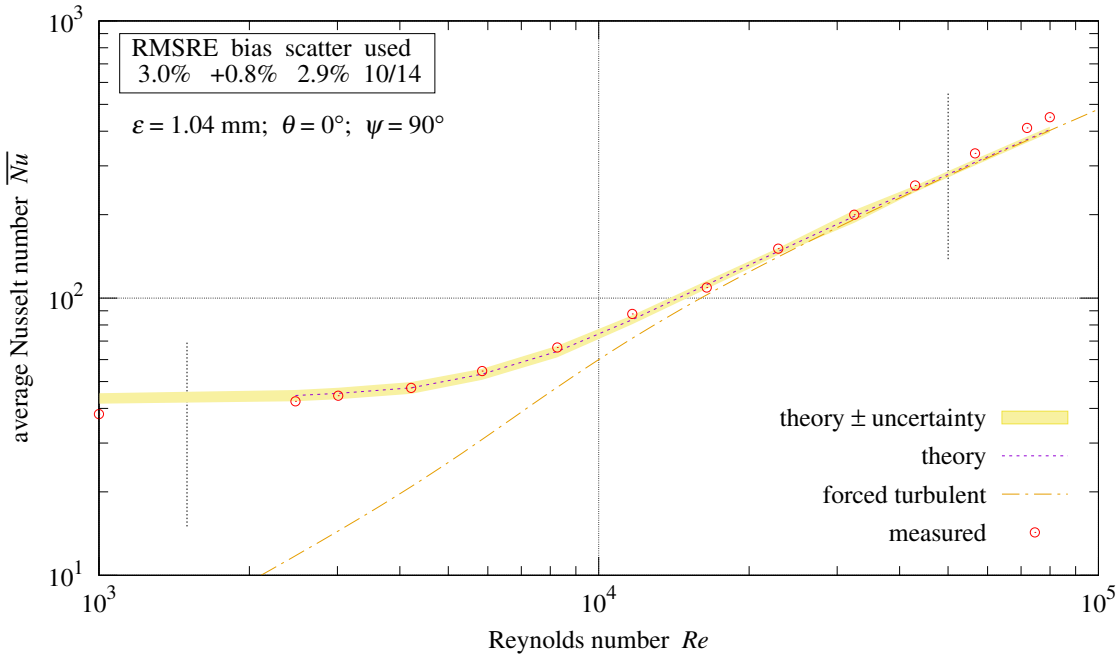

Figure 9 Vertical plate, horizontal forced flow, smooth turbulence

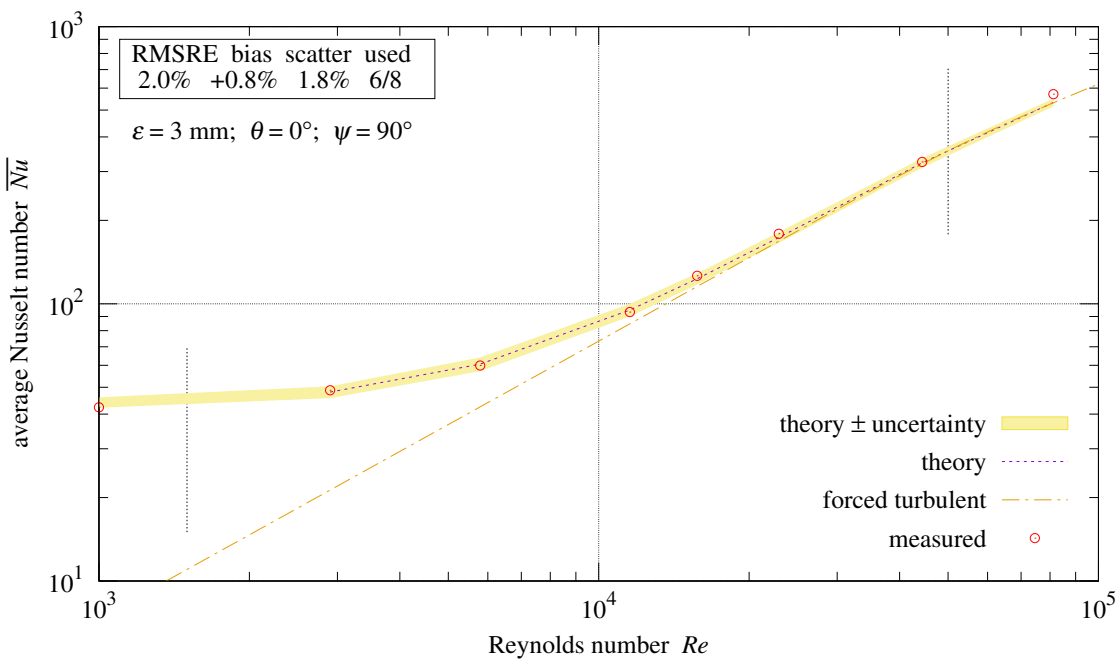

Figure 10 Vertical plate, horizontal forced flow, rough turbulence

5.3 **Vertical Plate With Forced Horizontal Flow.** Figure 1 shows that fluid is drawn horizontally towards the heated surface, then rising. Their heat flows are thus perpendicular, suggesting the ℓ^2-norm for combining $\overline{h_F}$ and vertical $\overline{h'}$:

$$\overline{h} = \left\| \overline{h_F}, \overline{h'} \right\|_2 \tag{14}$$

Figures 9 and 10 compare formula (14) with measurements of vertical plates in horizontal flow shedding forced smooth or forced rough turbulence, respectively.

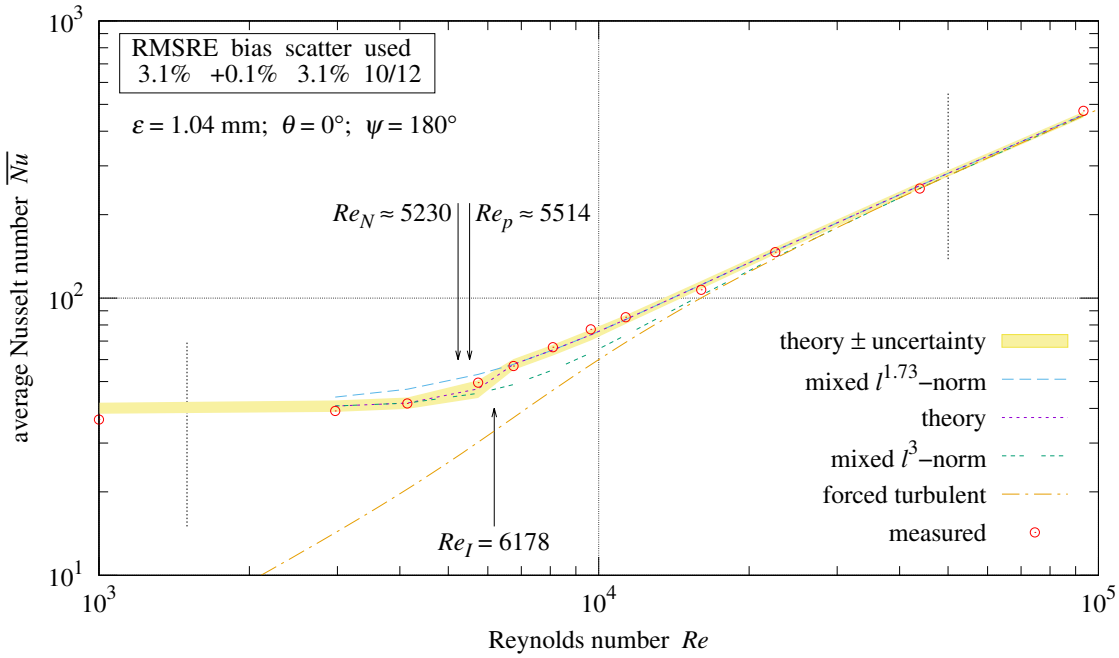

Figure 11 Vertical plate, opposing forced flow, smooth turbulence

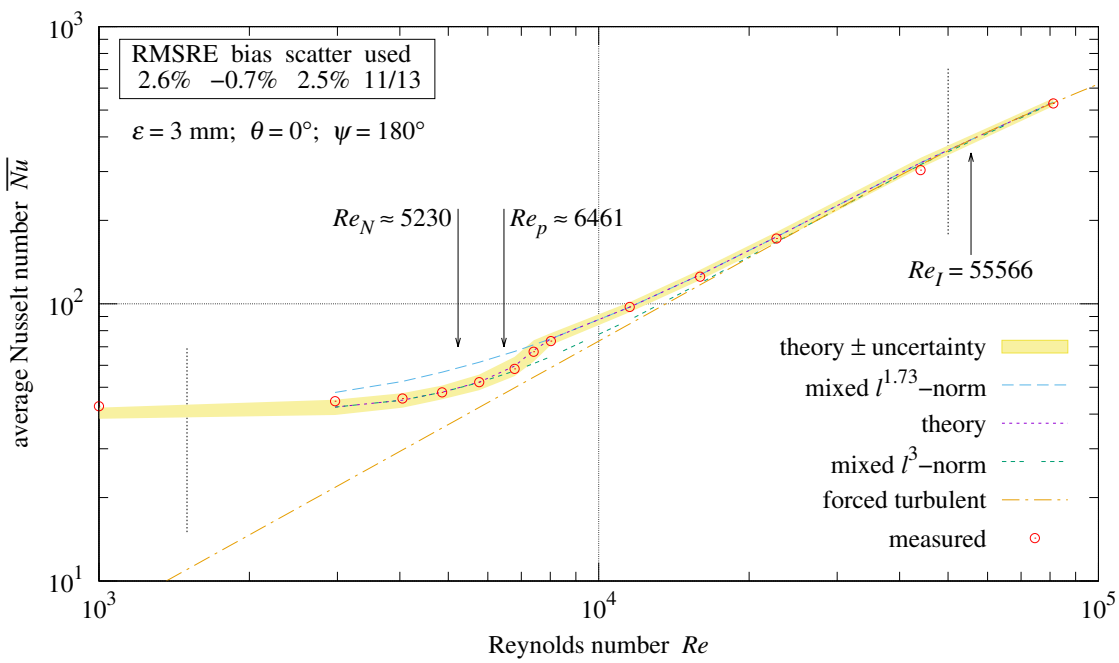

Figure 12 Vertical plate, opposing forced flow, rough turbulence

5.4 Vertical Plate With Forced Downward Flow.

The two flows are in opposite directions in the same channel. At low speeds their boundary layers overlap, such that these flows will compete for surface area. Table 2 shows that $\overline{Nu'}$ is proportional to $\sqrt[3]{Ra'}$, suggesting the ℓ^3-norm for combining $\overline{h'}$ and $\overline{h_F}$:

$$\overline{h} = \left\| \overline{h_F}, \overline{h'} \right\|_3 \tag{15}$$

At high speeds, a second boundary layer forms between the natural and forced flows, which serves to increase heat transport through the natural boundary layer, exceeding the ℓ^2-norm, but less than the

$\ell^{\sqrt{2}}$-norm. $p = \sqrt{3} \approx 1.732$ matches the data:

$$\overline{h} = \left\| \overline{h_F}, \overline{h'} \right\|_{\sqrt{3}} \tag{16}$$

The Re_N arrow indicates the approximate position of natural convection's effective Reynolds number calculated by formula (8). The Re_I arrow marks the transition from forced rough turbulent convection to smooth.

$$Re_p = {Re_N}^2 / Re_F(Re_N) = Re_N \exp_{C_W}\left(4 \exp_4\left(-[Re_N/Re_I]^4\right)\right) \qquad \exp_b(\varphi) \equiv b^{\varphi} \tag{17}$$

Re_p formula (17) is Re_N incorporating the formula (11) width correction; it marks the lower edge of the transition between $p = 3$ and $p = \sqrt{3}$.

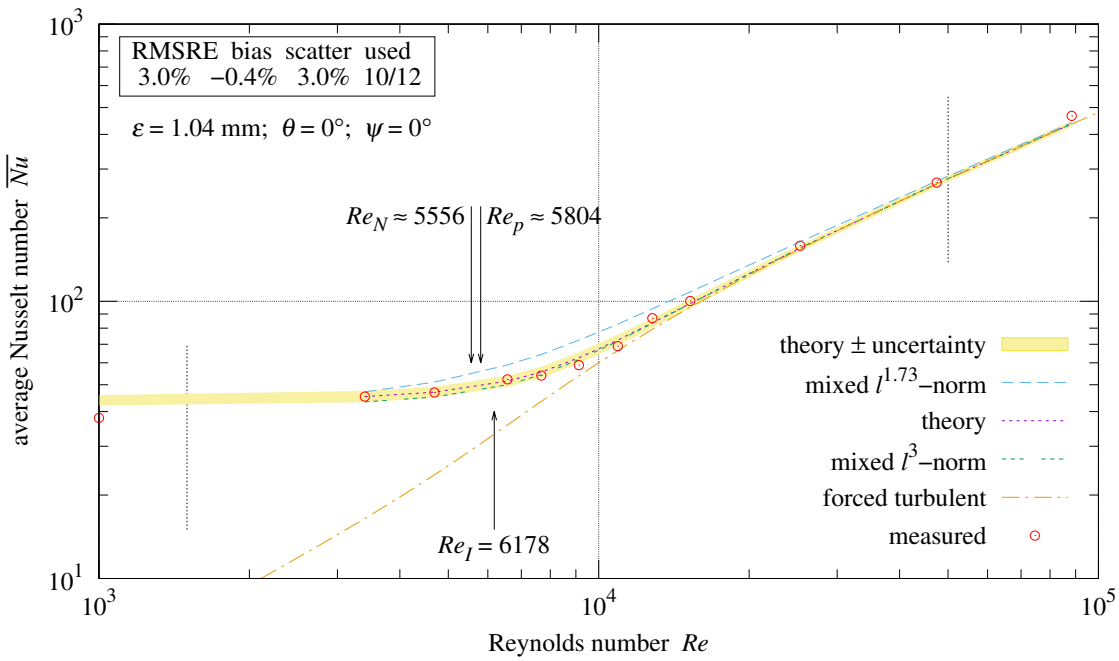

Figure 13 Vertical plate, aiding forced flow, smooth turbulence

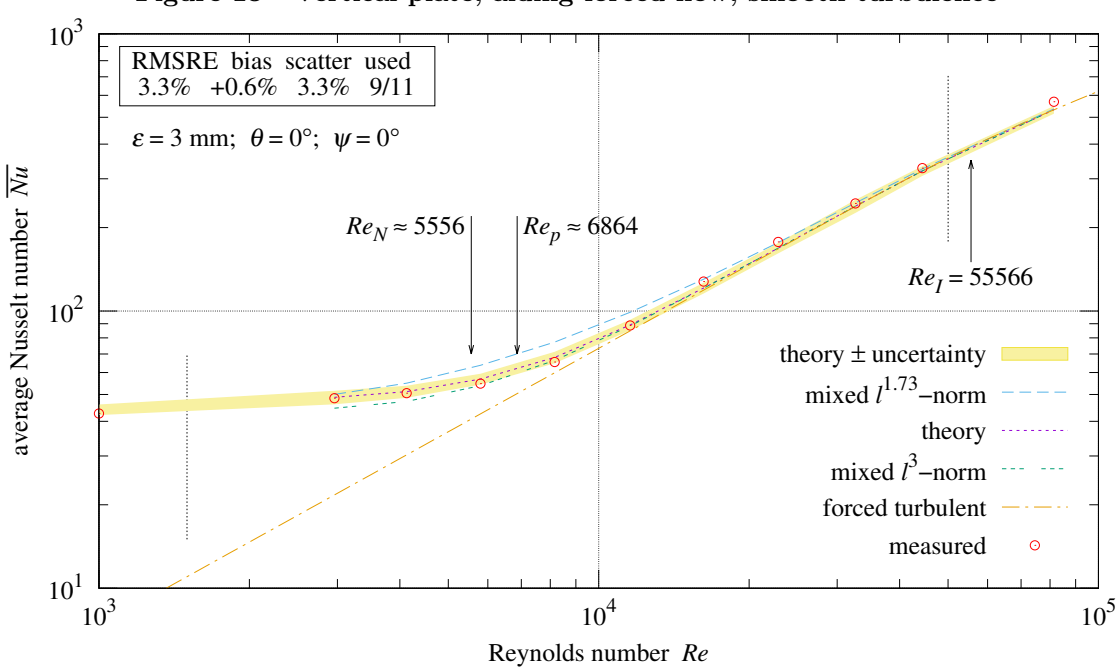

Figure 14 Vertical plate, aiding forced flow, rough turbulence

5.5 **Vertical Plate With Forced Upward Flow.** At low speeds, turbulent forced upward flow increases the natural convective heat transport, leading to $\overline{h} = \left\|\overline{h_F}, \overline{h'}\right\|_{\sqrt{3}}$. At high speeds however, the boundary layers are close to the plate, sharing the boundary layer fluid; the boundary layers thus compete for plate area, leading to $\overline{h} = \left\|\overline{h_F}, \overline{h'}\right\|_3$.

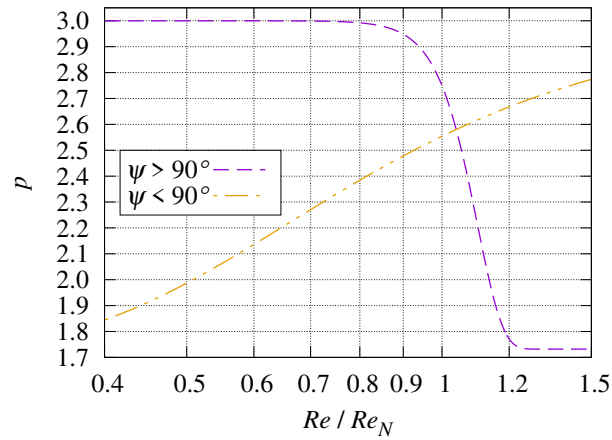

Figure 15 Vertical plate p versus Re/Re_p, ψ

Table 3 Corner cases p

Description	θ	ψ	p
upward facing plate	$-90.0°$	$90.0°$	2
aiding vertical plate	$+0.0°$	$0.0°$	$\exp_3\left(1/2 + \exp_2\left(-[Re_p/Re]^2/2\right)/2\right)$
vertical plate	$+0.0°$	$90.0°$	2
opposing vertical plate	$+0.0°$	$180.0°$	$\exp_3\left(1/2 + \exp_{16}\left(-[Re/Re_p]^{16}/16\right)/2\right)$
downward facing plate	$+90.0°$	$90.0°$	5

5.6 **Vertical Plate With Forced Flows at any Angle.** All vertical cases examined so far combine $\overline{h_N}$ and $\overline{h_F}$ using the ℓ^p-norm with $\sqrt{3} \le p \le 3$. However, p varies with Re in the vertical aiding and opposing cases. Needed is a function of Re which varies smoothly between asymptotes $\sqrt{3}$ and 3. This suggests raising 3 to an exponent between 1/2 and 1. With $\zeta > 1$ and $\varrho = Re/Re_p > 0$, ϱ^ζ/ζ varies between 0 and ∞; $\exp_\zeta\left(-\varrho^\zeta/\zeta\right)$ varies between 0 and 1. Formula (18) varies between $p = 3$ and $p = \sqrt{3}$, with sharpness controlled by ζ. The opposing flow transition is abrupt with $\zeta = 16$ and $\varrho = Re/Re_p$ and gradual for aiding flow with $\zeta = 2$ and $\varrho = Re_p/Re$.

$$p(\zeta, \varrho) = \exp_3\left(1/2 + \exp_\zeta\left(-\varrho^\zeta/\zeta\right)/2\right) \qquad \exp_b(\varphi) \equiv b^\varphi \tag{18}$$

Let ψ be the angle between the forced flow and the zenith. Figure 15 plots p at $\zeta = 2$ and $\zeta = 16$, used with $\psi = 0°$ and $\psi = 180°$, respectively. Table 3 lists p for horizontal and vertical plate and flows.

The theory curve and error statistics in Figures 11, 12, 13, and 14 are of formula (18).

At $\psi = 0°$, the forced and natural flows align. As ψ tilts toward horizontal ($\pm 90°$), the forced flow can be split into components aligned and perpendicular to the natural upward flow. The coefficients of these components are trigonometric functions of ψ. Tilting to the left or right of $\psi = 0$ by equal angles must transfer the same amount of heat. Thus, the trigonometric coefficients must be even functions ($F(\psi) = F(-\psi)$) of ψ; $[\sin\psi]^2$ and $[\cos\psi]^2$ are even functions, leading to the first line of formula (19), where $\overline{h'_\theta} \equiv \overline{h'}(|\cos\theta|\, Ra'/\Xi)$.

Downward tilted flow requires a sharper transition around $\psi = 180°$, implemented using $[\sin\psi]^4$ and $[\cos\psi]^4$ as the coefficients in the second line of formula (19).

$$\overline{h_\theta} = \begin{cases} [\sin\psi]^2 \left\|\overline{h_F}, \overline{h'_\theta}\right\|_2 + [\cos\psi]^2 \left\|\overline{h_F}, \overline{h'_\theta}\right\|_{p(2, Re_p/Re)}, & \text{if } \psi < 90°; \\ [\sin\psi]^4 \left\|\overline{h_F}, \overline{h'_\theta}\right\|_2 + [\cos\psi]^4 \left\|\overline{h_F}, \overline{h'_\theta}\right\|_{p(16, Re/Re_p)}, & \text{otherwise.} \end{cases} \tag{19}$$

5.7 **Mixed Convection From an Inclined Plate.** Mixed convection from an inclined plate is calculated by replacing each horizontal and vertical natural convection function in formula (7) with its mixture ℓ^p-norm:

$$\overline{h} = \begin{cases} \max\left(\overline{h_\theta}, \left\|\overline{h_F}, \overline{h^*}(|\sin\theta|\, Ra^*)\right\|_2\right) & 0^\circ \le \theta \le +90^\circ \\ \max\left(\overline{h_\theta}, \left\|\overline{h_F}, \overline{h_R}\,(|\sin\theta|\, Ra_R/\Xi)\right\|_5\right) & -90^\circ \le \theta \le 0^\circ \end{cases} \tag{20}$$

With $\overline{h_F} = 0$, mixed formula (20) simplifies to natural formula (7).
When θ and ψ are multiples of 90°, formula (20) simplifies to $\left\|\overline{h_F}, \overline{h_N}\right\|_p$, with p from Table 3.

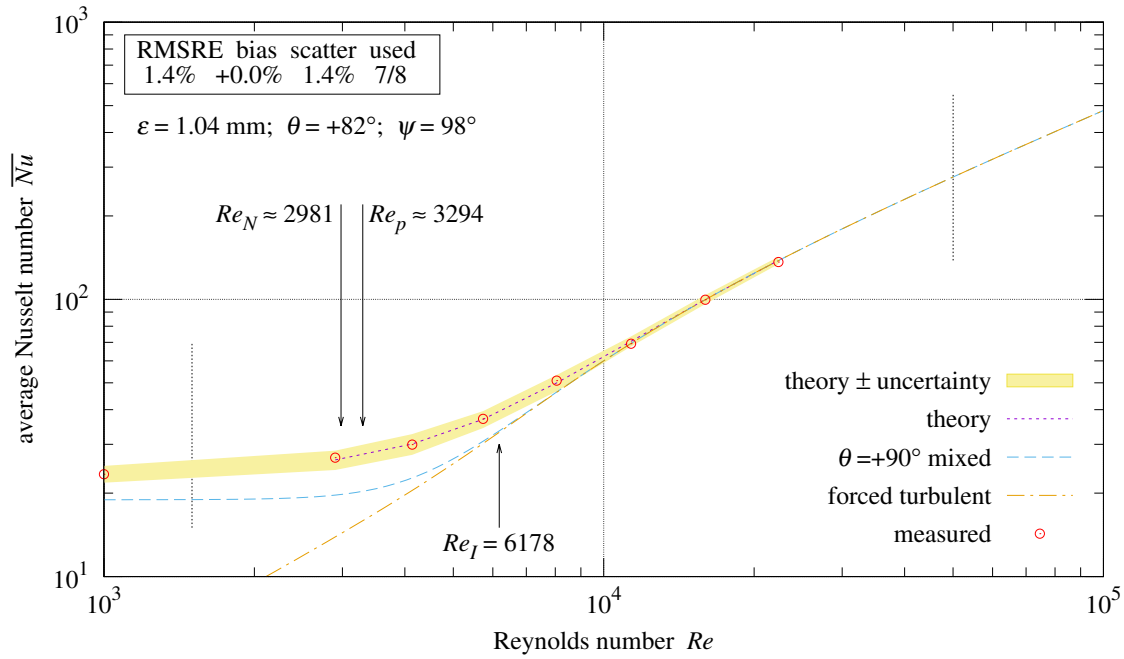

Figure 16 Inclined plate, $\theta = +82°$, forced opposing, smooth turbulence

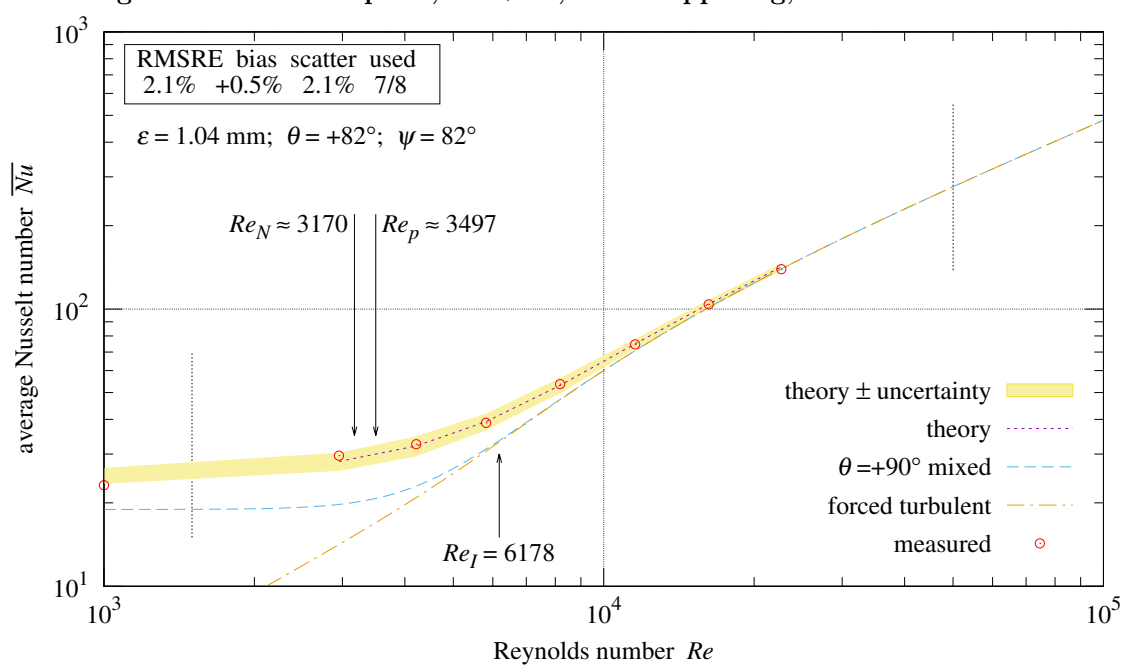

Figure 17 Inclined plate, $\theta = +82°$, forced aiding, smooth turbulence

Figure 16 shows forced flow opposing natural convection at $\theta = +82$ with $\psi = 98°$. Figure 17 shows forced flow aiding natural convection at $\theta = \psi = +82°$. The $\theta = \psi = +90°$ curve is shown for comparison.

6. Results

Tables 4 and 5 summarize the present theory's conformance with 104 measurements in twelve data-sets from the present apparatus's two plates. The 3 mm roughness data-sets have RMSRE values between 2.0% and 3.8%; The 1 mm roughness data-sets have RMSRE values between 1.4% and 3.1%. The smaller RMSRE values of the 1 mm plate may reflect improvements in fan rotation variability.

Table 4 Convection measurements versus present theory, rough turbulence

Description	ε	θ	ψ	RMSRE	Bias	Scatter	Used
downward facing plate	3.00 mm	+90.0°	90.0°	3.8%	+1.0%	3.7%	10/14
upward facing plate	3.00 mm	−90.0°	90.0°	3.6%	−0.2%	3.6%	6/10
vertical plate	3.00 mm	+0.0°	90.0°	2.0%	+0.8%	1.8%	6/8
opposing vertical plate	3.00 mm	+0.0°	180.0°	2.6%	−0.7%	2.5%	11/13
aiding vertical plate	3.00 mm	+0.0°	0.0°	3.3%	+0.6%	3.3%	9/11

Table 5 Convection measurements versus present theory, smooth turbulence

Description	ε	θ	ψ	RMSRE	Bias	Scatter	Used
downward facing plate	1.04 mm	+90.0°	90.0°	2.6%	−0.5%	2.6%	12/15
upward facing plate	1.04 mm	−90.0°	90.0°	2.5%	+0.2%	2.5%	6/8
vertical plate	1.04 mm	+0.0°	90.0°	3.0%	+0.8%	2.9%	10/14
opposing vertical plate	1.04 mm	+0.0°	180.0°	3.1%	+0.1%	3.1%	10/12
aiding vertical plate	1.04 mm	+0.0°	0.0°	3.0%	−0.4%	3.0%	10/12
opposing inclined plate	1.04 mm	+82.0°	98.0°	1.4%	+0.0%	1.4%	7/8
aiding inclined plate	1.04 mm	+82.0°	82.0°	2.1%	+0.5%	2.1%	7/8

7. Discussion

An unobstructed plate induces a single steady-state mode of natural convection (face up, down, or vertical). The instances of max() in formula (7) choose the largest surface conductance among these modes. Similarly, instances of max() in formula (20) choose the largest surface conductance among each natural convection mode mixed with $\overline{h_F}$ using the ℓ^p-norm.

The fan forcing air through the chamber is sufficient to counter the effect of the wind-tunnel's obstructions to horizontal flow, except in the case of the vertical plate with opposing flow. In order to draw some air upward at slow (downward) fan speeds, the air's momentum must be reversed. This is modeled by increasing parameter B of Table 2 by twice the vertical distance from the plate to the test chamber upper edge, normalized by L and the ratio of the upper edge perimeter to the plate width.

With the fan stopped, the natural convection measurement (plotted at $Re = 10^3$ in the graphs) is lower than predicted by formula (5) when the walls of the test chamber partially obstruct buoyancy-induced fluid flows.

7.1 Laminar Mixed Convection.

This investigation argues that use of the $\ell^{\sqrt{3}}$-norm with vertical plates is due to turbulent flow. This implies that laminar mixed convection must differ from turbulent. Lin et al. [5] employs the ℓ^4-norm for laminar mixed flow from downward-facing and vertical aiding plates.

7.2 Effective Vertical Reynolds Number.

Aiding and opposing vertical plate measurements in a fluid other than air are needed to further test the effective vertical Reynolds number, Re_N formula (8).

8. Conclusions

The average mixed convective surface conductance, $\overline{h}$, is:

$$\overline{h} = \begin{cases} \max\left(\overline{h_\theta}, \left\|\overline{h_F}, \overline{h^*}(|\sin\theta|\, Ra^*)\right\|_2\right) & 0^\circ \le \theta \le +90^\circ \\ \max\left(\overline{h_\theta}, \left\|\overline{h_F}, \overline{h_R}\left(|\sin\theta|\, Ra_R/\Xi\right)\right\|_5\right) & -90^\circ \le \theta \le 0^\circ \end{cases}$$

$$\overline{h_\theta} = \begin{cases} [\cos\psi]^2 \left\|\overline{h_F}, \overline{h'_\theta}\right\|_{p(2, Re_p/Re)} + [\sin\psi]^2 \left\|\overline{h_F}, \overline{h'_\theta}\right\|_2, & \text{if } \psi < 90^\circ; \\ [\cos\psi]^4 \left\|\overline{h_F}, \overline{h'_\theta}\right\|_{p(16, Re/Re_p)} + [\sin\psi]^4 \left\|\overline{h_F}, \overline{h'_\theta}\right\|_2, & \text{otherwise.} \end{cases}$$

$$p(\zeta, \varrho) = \exp_3\left(1/2 + \exp_\zeta\left(-\varrho^\zeta/\zeta\right)/2\right)$$

$$\overline{h'_\theta} = \overline{h'}(|\cos\theta|\, Ra'/\Xi) \qquad Re_p = Re_N \exp_{C_W}\left(4\, \exp_4\left(-[Re_N/Re_I]^4\right)\right)$$

$$C_W = \|1, \varepsilon/L_W\|_{\sqrt{1/2}} \qquad \|y, z\|_p \equiv [\ |y|^p + |z|^p]^{1/p} \qquad \exp_b(\varphi) \equiv b^\varphi$$

$$\Xi \equiv \left\|1\ ,\ \frac{0.5}{Pr}\right\|_{\sqrt{1/3}} \qquad Re_N \approx \frac{8\,\overline{Nu'}\,\Xi^3}{Nu'_0} \qquad \overline{Nu'} \equiv \frac{\overline{h'}\,L}{k} \qquad Nu'_0 \equiv \frac{2^4}{\sqrt[4]{2}\,\pi^2}$$

The present theory was compared with 104 measurements in twelve data-sets from the present apparatus. The twelve data-sets have RMSRE values between 1.4% and 4% relative to the present theory.

9. Nomenclature

C_W	rough turbulent plate width correction factor
$\overline{h}$	average convective surface conductance (W/(m^2 · K))
$\overline{h_F}$	forced convective surface conductance (W/(m^2 · K))
$\overline{h_N}$	natural convective surface conductance (W/(m^2 · K))
$\overline{h^*}$	upward natural convective surface conductance (W/(m^2 · K))
$\overline{h'}$	vertical plate natural convective surface conductance (W/(m^2 · K))
$\overline{h'_\theta}$	vertical component of natural convective surface conductance (W/(m^2 · K))
$\overline{h_\theta}$	vertical component of inclined natural convective surface conductance (W/(m^2 · K))
$\overline{h_R}$	downward natural convective surface conductance (W/(m^2 · K))
k	fluid thermal conductivity (W/(m · K))
L	characteristic length (m)
L_W	width of plate (m)
$\overline{Nu}$	average Nusselt number
$\overline{Nu'}$	average Nusselt number of vertical plate natural convection
Nu'_0	Nusselt number of vertical plate conduction
p	exponent in ℓ^p-norm
Pr	Prandtl number of the fluid
Ra	Rayleigh number
Ra'	vertical plate Rayleigh number
Ra^*	upward Rayleigh number
Ra_R	downward Rayleigh number
Re	Reynolds number of the forced flow parallel to the plate
Re_I	Reynolds number of rough turbulent transition to smooth turbulence
Re_N	effective Reynolds number of vertical natural convection
Re_p	effective Reynolds number of vertical natural convection scaled by C_W

9.1 Greek Symbols.

ψ	angle between the forced flow and the zenith; 0° is aiding flow; 180° is opposing flow
θ	angle of the plate surface from vertical; face up is −90°; face down is +90°
ε	surface RMS height-of-roughness (m)
Ξ	natural convection self-obstruction factor

Supplementary Materials

A zip archive of PDF files of graphs and estimated measurement uncertainties of each 102-minute time-series producing a convection measurement can be downloaded from:

`http://people.csail.mit.edu/jaffer/convect`

Acknowledgments

Thanks to Roberta Jaffer for assistance and problem-solving suggestions.

Abbreviations

The following abbreviations are used in this manuscript:

RMS	root-mean-squared	$\sqrt{\sum_{i=1}^{n} x_i^2/n}$
RMSRE	root-mean-squared relative error	
RSS	root-sum-squared	$\sqrt{\sum_i x_i^2}$

10. References

[1] Aubrey Jaffer. Skin-Friction and Forced Convection from Rough and Smooth Plates. *ArXiv e-prints*, October 2020, doi:10.48550/ARXIV.1810.05743.

[2] Aubrey Jaffer. Natural convection heat transfer from an isothermal plate. *Thermo*, 3(1):148–175, 2023, doi:10.3390/thermo3010010.

[3] S. W. Churchill and R. Usagi. A general expression for the correlation of rates of transfer and other phenomena. *AIChE Journal*, 18(6):1121–1128, 1972, doi:10.1002/aic.690180606.

[4] Hermann Schlichting. *Boundary-Layer Theory*. McGraw Hill, New Delhi, seventh edition, 2014. Translated by Kestin, J.

[5] HT Lin, WS Yu, and CC Chen. Comprehensive correlations for laminar mixed convection on vertical and horizontal flat plates. *Wärme-und Stoffübertragung*, 25(6):353–359, 1990.

[6] Tetsu Fujii and Hideaki Imura. Natural-convection heat transfer from a plate with arbitrary inclination. *International Journal of Heat and Mass Transfer*, 15(4):755–764, 1972, doi:10.1016/0017-9310(72)90118-4.

[7] T Aihara, Y Yamada, and S Endö. Free convection along the downward-facing surface of a heated horizontal plate. *International Journal of Heat and Mass Transfer*, 15(12):2535 – 2549, 1972, doi:10.1016/0017-9310(72)90145-7.

[8] X. A. Wang. An experimental study of mixed, forced, and free convection heat transfer from a horizontal flat plate to air. *Journal of Heat Transfer*, 104(1):139–144, 1982, doi:10.1115/1.3245040.

[9] J. H. Lienhard, IV and J. H. Lienhard, V. *A Heat Transfer Textbook*. Phlogiston Press, Cambridge, MA, 5th edition, August 2020. Version 5.10.